ADVANCED PHOTONICS RESEARCH Open Access
www.adpr-journal.com

Fluorine-Enhanced Room Temperature Luminescence of Er-Doped Crystalline Silicon

Xiaoming Wang, Jiajing He, Shenbao Jin, Huan Liu, Hongkai Li, Huimin Wen, Xingyan Zhao, Roozbeh Abedini-Nassab, Gang Sha, Fangyu Yue, and Yaping Dan**

The silicon-based light-emitting devices are the bottleneck of fully integrated silicon photonics. Doping silicon with erbium (often along with oxygen) is an attractive approach to turn silicon into a luminescent material, which has been explored for decades. One of the main challenges is the strong thermal quenching effect that results in weak photoluminescence (PL) efficiency. Herein, it is shown that the co-doping of fluorine with erbium ions can significantly suppress the thermal quenching effect and Auger recombination, resulting in a three-order-of-magnitude increase in PL compared to Er/O-doped crystalline silicon. As a result, relatively strong PL is observed from fluorine-doped silicon at room temperature.

1. Introduction

Silicon photonics will speed up the computing and data transmission of the current communication network by integrating optical and electronic devices on the same silicon substrate.[1–4] This technology requires efficient silicon-based light sources and optical amplifiers at communication wavelengths.[4–6] However, silicon is an indirect band gap semiconductor, which cannot efficiently emit light at communication wavelengths. In the past several decades, significant efforts have been devoted to developing efficient silicon-based light-emitting materials, including III–V quantum dots and strained Ge, epitaxially grown on silicon.[7–12] Doping silicon with erbium ions is the earliest effort to create luminescent silicon, which is also one of the most attractive approaches[13,14] as it is compatible with complementary metal oxide semiconductor (CMOS) processes. However, it suffers from strong thermal quenching in photoluminescence (PL), resulting in an extremely low efficiency at room temperature (RT).[14–18] Interestingly, our group[19] recently found that the thermal quenching effect can be suppressed by employing a deep cooling process to treat the Er/O co-doped crystalline silicon, as a result of which the PL efficiency at RT is improved by two orders of magnitude. The improvement is due to the fact that the deep cooling process can mitigate the precipitation of erbium ions into Er-O-Si nanocrystals that often occurs in the slow cooling process of standard rapid thermal annealing (RTA). Without the Er/O precipitation into large nanocrystals, the nonradiative emission paths through the interface states between nanocrystalline precipitates and silicon crystal are thus eliminated, resulting in a weak thermal quenching effect in PL. In this work, we surprisingly found that the thermal quenching effect can also be suppressed by co-doping fluorine (F) ions with erbium ions, although Er/F ions have precipitated into large nanocrystals with the standard RTA treatment. It is likely because F ions can passivate the interface states between erbium nanocrystals and Si lattice.

X. Wang, J. He, H. Liu, H. Wen, X. Zhao, Y. Dan
University of Michigan-Shanghai Jiao Tong University Joint Institute
Shanghai Jiao Tong University
Shanghai 200240, China
E-mail: jiajinghe@sjtu.edu.cn; yaping.dan@sjtu.edu.cn

J. He
Laboratory of Micro-Nano Optoelectronic Materials and Devices
Shanghai Institute of Optics and Fine Mechanics
Chinese Academy of Sciences
Shanghai 201800, China

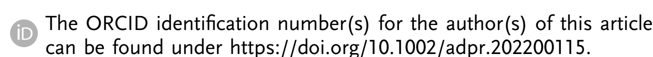
The ORCID identification number(s) for the author(s) of this article can be found under https://doi.org/10.1002/adpr.202200115.

© 2022 The Authors. Advanced Photonics Research published by Wiley-VCH GmbH. This is an open access article under the terms of the Creative Commons Attribution License, which permits use, distribution and reproduction in any medium, provided the original work is properly cited.

DOI: 10.1002/adpr.202200115

J. He
CAS Center for Excellence in Ultra-intense Laser Science
Shanghai Institute of Optics and Fine Mechanics
Chinese Academy of Sciences
Shanghai 201800, China

S. Jin, G. Sha
School of Materials Science and Engineering
Herbert Gleiter Institute of Nanoscience
Nanjing University of Science and Technology
Nanjing 210094, China

H. Li, F. Yue
Key Laboratory of Polar Materials and Devices
Ministry of Education
East China Normal University
Shanghai 200241, China

R. Abedini-Nassab
Faculty of Mechanical Engineering
Tarbiat Modares University
P. O. Box: 14115-111, Tehran, Iran

2. Results and Discussion

The intrinsic <100> single crystalline silicon (FZ) wafer was first cleaned with acetone and deionized water, piranha solution (sulfuric acid: 30% hydrogen peroxide = 3:1) followed for 20 min at 100 °C, and rinsed in deionized water. O and F ions were implanted separately into different samples with a dose of 1×10^{16} cm^{-2} at 30 keV to create Er/O and Er/F samples for comparison. Erbium ions were implanted with a dose of 4×10^{15} cm^{-2} at 200 keV. After the implantation, the samples were cut into small pieces and went through the cleaning procedure again. RTA process (900 °C for 5 min) was applied to activate the implanted atoms and repair the lattice damage caused by ion implantation.

PL spectra and decay curves of the Er/F: Si sample excited by a blue laser with a diameter of 1.5 mm ($\lambda = 405$ nm) were recorded at different temperatures to investigate the thermal quenching effect and the back-transfer dynamics. For comparison, the Er/O:Si sample was also measured since the Er/O:Si samples are the most widely studied. As shown in **Figure 1**a, no PL is observed in the Er/O:Si samples at RT. For the Er/F: Si sample, the PL spectrum peaked at 1532 nm with a full width half maximum (FWHM) of 40 nm is acquired at RT, as shown in Figure 1a. The PL peak of the Er/F samples is blue-shifted and broadened, likely because the local environment of Er ions is changed by binding with F instead of O. As known, for the Er-doped silicon, strong thermal quenching is one of the main factors that result in the low RT luminescence efficiency. As shown previously, Er-O-Si composites will precipitate as nanocrystals in the crystalline silicon. The lattice mismatch between the nanocrystals and crystalline Si will create a high concentration of interface defects, resulting in strong nonradiative recombination, which can be suppressed at low temperatures.[13] For this reason, it is not surprising that the PL intensity of Er/O doped Si is quenched by more than three orders of magnitude as the temperature increases from 77 to 300 K (Figure 1b), which is widely observed in literatures.[17,18,20] Surprisingly, the Er/F: Si sample treated by the same RTA process exhibits strong PL emission which is nearly independent of temperature, shown as the red squares in Figure 1b (only quenched by 3 times from 77 to 300 K). In addition, the Er/F:Si sample exhibits a stronger low temperature PL intensity by one order of magnitude than the Er/O:Si sample. It is likely because the Er/F:Si sample has a higher Er optical activation rate. Clearly, F dopants play an important role that is completely different from O dopants.

To better understand the role of F ions, transient PL decay curves at the peak wavelength were recorded at a pump power of 200 mW as the temperature was lowered from RT to 77 K (Figure S1, Supporting Information). The PL decay traces for both Er/F and Er/O samples can be well described with a double exponential function as in Equation (1)

$$I(t) = I_{\text{fast}} e^{-\frac{t}{\tau_{\text{fast}}}} + I_{\text{slow}} e^{-\frac{t}{\tau_{\text{slow}}}} \quad (1)$$

where τ_{fast} and τ_{slow} are decay times for the fast and slow components, respectively. I_{fast} and I_{slow} are the corresponding fractional contribution. The nonexponential decay behavior suggests at least two relax/recombination channels related to Er states.

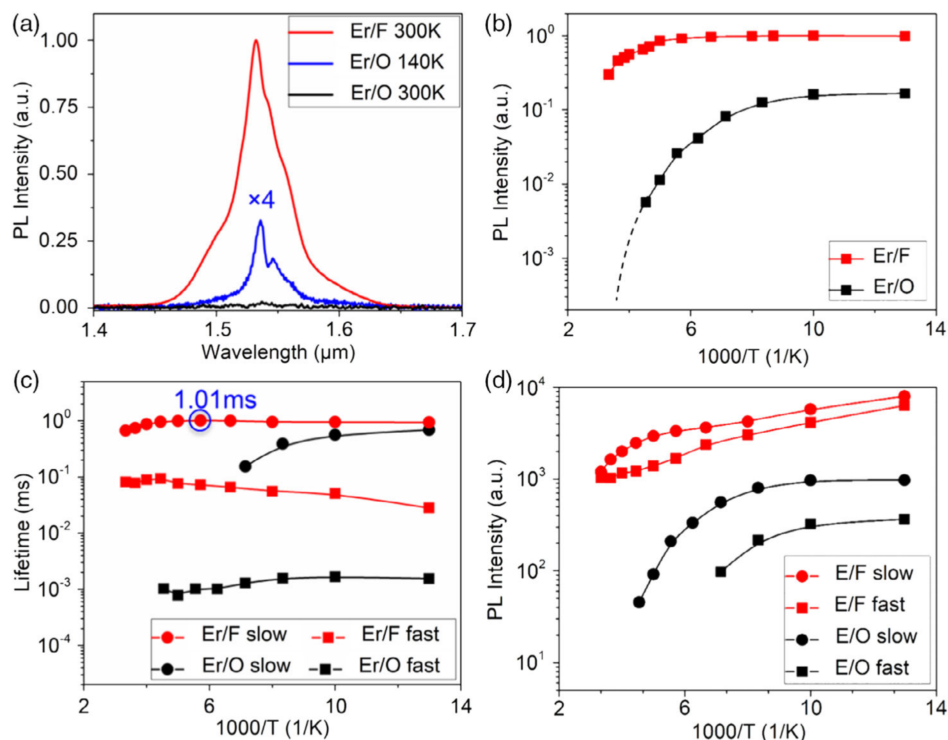

Figure 1. Temperature-dependent steady and transient analysis for Er/F-doped Si and Er/O-doped Si samples. a) PL spectra of Er/F-Si and Er/O-Si at different temperatures. b) Steady-state PL intensity. c) Fast and slow lifetimes of carriers for Er-doped Si with F (red) and O (black), respectively. The excitation laser was at 405 nm with a power of 200 mW. d) PL intensity of the fast and slow component for the Er/O:Si and Er/F:Si samples.

© 2022 The Authors. Advanced Photonics Research published by Wiley-VCH GmbH

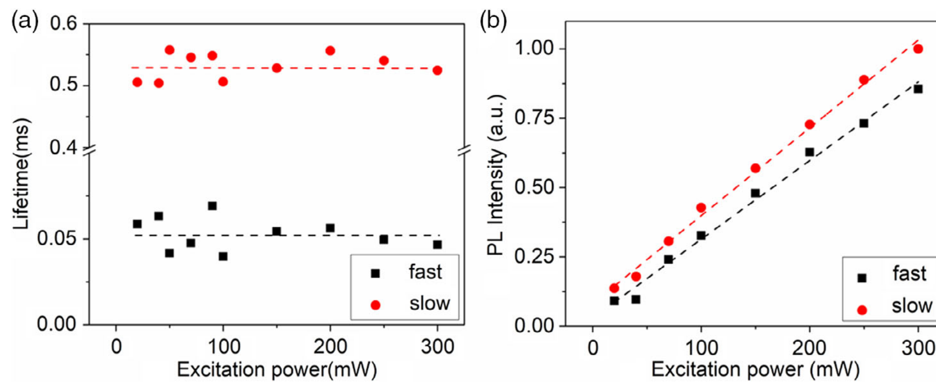

Figure 2. Power-dependent transient analysis for the Er/F:Si sample at 300 K. a) Excitation-dependent fast and slow decay times. b) Excitation-dependent PL intensity of fast and slow components, respectively.

The extracted lifetimes and PL intensities were shown in Figure 1c,d, respectively. For the Er/O: Si sample, τ_{fast} is quite short (≈1 μs), two orders of magnitude fast than the general lifetime of Er ion luminescence, which could be related to the non-recombination process, e.g., the fast relaxation or back-transfer to the lower or higher energy levels, or even the Auger recombination. However, τ_{slow}, which is highly dependent on temperature and decreases from 690 to 155 μs when the temperature goes up from 77 to 140 K, could be related to the lifetime of carriers related to the Er ion luminescence. In contrast, the lifetimes of the Er/F:Si are much larger and nearly independent of temperature. The slow and fast time constant is ≈1 ms and 30–100 μs, respectively.

The radiative recombination lifetimes for Er/O: Si and Er/F: Si samples are the same, since the electronic transition occurs in the inner orbitals of Er ions which are less affected by the environment. The PL intensity is proportional to the excited Er concentration. The weak RT PL for the Er/O doped silicon is attributed to a number of factors, including the low concentration of optical active Er, high concentration of nonradiative recombination centers and strong temperature quenching for carrier lifetime.[13,21–24] In contrast, Er/F-doped samples have a much stronger PL which comes along with longer lifetimes and weaker dependence on temperature. In addition, both fast and slow carrier lifetimes exhibit an anomalous temperature dependence. As the temperature goes up, the lifetime of the slow decay

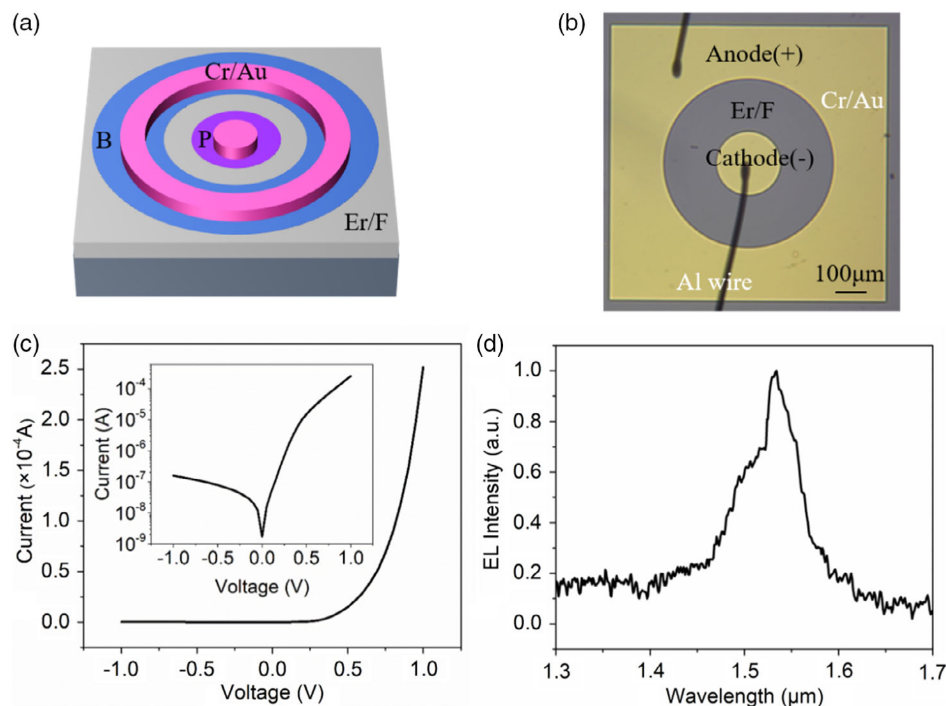

Figure 3. Er/F:Si LED device. a) 3D structure of the device. b) Schematic of the device. c) *I–V* curve. Inset: logarithm current versus bias. d) RT EL spectrum.

© 2022 The Authors. Advanced Photonics Research published by Wiley-VCH GmbH

component increases, reaching the maximum value of ≈1 ms at 175 K. Similar behaviors have been reported and ascribed to the carriers delocalizing from trap states or defect states to excited states and Auger effect is weak.[25,26] It only decays by three times with temperature increasing from 77 to 300 K. The incorporation of F ions increases the intensity of fast and slow components by at least one order of magnitude (Figure 1d). Thermal quenching can be effectively reduced, which means the probability of back transfer is decreased.

Another factor that limits the PL intensity is the Auger effect and nonradiative recombination via defects. Electrical measurements show that Er/O:Si samples have much lower sheet resistances than the Er/F:Si ones, indicating a high concentration of free electrons in the former. Therefore, Er/O:Si samples will have stronger Auger recombination at high injection. Indeed, for the Er/F:Si sample, Auger effect is negligible, because the lifetimes for the Er/F:Si sample are almost independent of the excitation power as shown in **Figure 2**a. As a result, the PL intensity of these two components is almost linear with the pumping power changing within about two orders of magnitude (Figure 2b). It is not difficult to conclude that the incorporation with F, in comparison with co-doped with O, can efficiently suppress the Auger effect and nonradiative recombination via defects.

The Er/F:Si sample was further fabricated into a light-emitting diode (LED). The sheet resistance of Er/F:Si is 7.3 kΩ sq^{-1}. Thus, boron (blue region) and phosphorus (purple region) were implanted to form the p-type and n-type region with a dosage of 1×10^{15} cm^{-2} at 20 keV and 1×10^{14} cm^{-2} at 60 keV, respectively (**Figure 3**a). The RTA process was employed to activate the dopants at the same time. A pair of co-axial metal electrode patterns were defined, followed by thermal evaporation of 5 nm Cr and 70 nm Au (Optical microscopic image of the device is shown in Figure 3b). The *I–V* curve exhibits a rectifying behavior of a typical PN junction diode with an on/off ratio of ≈3 orders of magnitude (Figure 3c). The ideal factor can be calculated as ≈2,

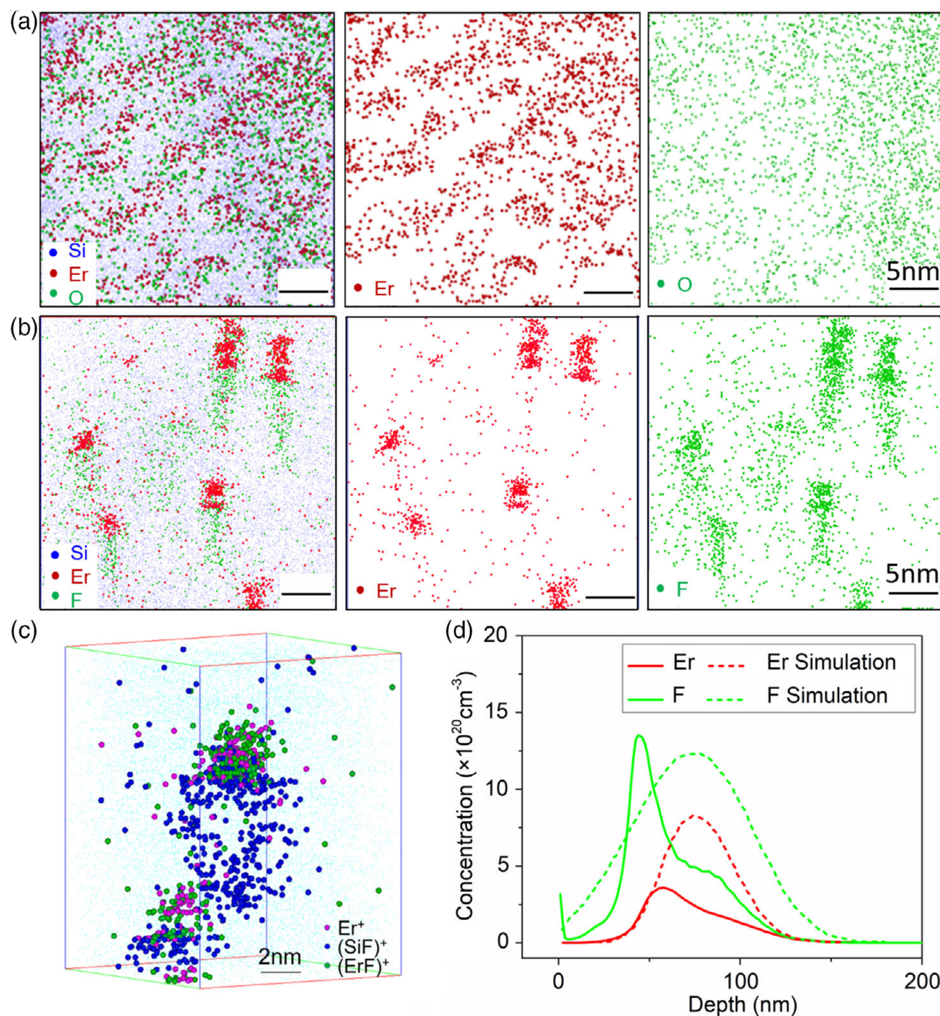

Figure 4. APT characteristic. a) The spatial distribution of Er and O atoms in the Er/O:Si sample treated by RTA. b) The spatial distribution of Er and F atoms in the Er/F:Si sample treated by RTA. c) Three-dimensional reconstruction volume with aggregations in the Er/F:Si sample. $(SiF)^+$ refers to SiF and SiF_2. $(ErF)^+$ refers to ErF and ErF_2. d) SIMS characterization of the RAT treated Er/F:Si sample. Ion distribution profiles of experimental results (solid line) and comparing them to simulation results (dashed lines).

© 2022 The Authors. Advanced Photonics Research published by Wiley-VCH GmbH

indicating that a high-quality PN junction diode is made and that electrons from the n^+ region and holes from the p^+ region dominantly recombine within the depletion region. The EL spectrum was measured by a cooled Ge detector with a peak of 1534 nm under the pulse operation condition, as shown in Figure 3d.

To better understand the luminescence mechanism, APT was used to map the spatial distribution of elements for both Er/O:Si and Er/F:Si samples. For the Er/O:Si sample, Er ions are clearly aggregated into "stripes" while O atoms are more uniformly distributed (**Figure 4**a). In contrast, both Er and F ions in the Er/F sample precipitate into clusters (Figure 4b). Three-dimensional reconstruction volume of Er and F atoms in Er/F:Si sample is shown in Figure S2, Supporting Information. A closer look at one of the clusters (Figure 4c) indicates that F atoms form larger clusters, wrapping around Er precipitates in the form of Er-F composites. This picture is largely consistent with the fact that F ions likely play a passivation role which leads to a weak thermal quenching effect and a low dark current of the fabricated PN junction.[27,28]

The Er and F atom distribution profiles of the Er/F:Si sample treated by RTA acquired by secondary ion mass spectroscopy (SIMS) are shown in Figure 4d. Compared with the calculated results, the peak positions of Er and F both shift toward the surface of Si, consistent with the fact that Er–F complexes are formed after annealing.[29,30] This observation is in line with previous reports[31,32] that F atoms migrate toward the surface at a temperature beyond 550 °C.

3. Conclusion

We have demonstrated that F has a passivation effect and can enhance the PL of Er-doped Si. In comparison with O dopants, F ions are more mobile and tend to aggregate with Er, potentially passivating defects on the surface of Er precipitates. As a result, the nonradiative recombinations including phonon-assisted relaxation and the Auger effect are suppressed. Unfortunately, the quantum efficiency of the Er/F:Si device is still relatively low due to the low activation rate of Er ions which we plan to improve in the future by exploring novel methods.

Supporting Information

Supporting Information is available from the Wiley Online Library or from the author.

Acknowledgements

X.M.W. and J.J.H. contributed equally to this work. This work was supported by the "Innovative Research Plan," Shanghai Municipality Bureau of Education (2019-01-07-0002-E00075), China National Postdoctoral Program for Innovative Talents (BX20200205), and the National Science Foundation of China (61904102). SB.J. and G.S. would like to acknowledge facility use and scientific and technical assistance from the Materials Characterization Facility in Nanjing University of Science and Technology. The authors are grateful for the support for PL analysis by Dr. Ruibin Wang at Instrumental Analysis Center of Shanghai Jiao Tong University. The devices were fabricated at the Center of Advanced Electronic Materials and Devices (AEMD) Shanghai Jiao Tong University.

Conflict of Interest

The authors declare no conflict of interest.

Data Availability Statement

The data that support the findings of this study are available from the corresponding author upon reasonable request.

Keywords

Auger recombination, Er-doped Si, light emission devices, silicon-based light source, thermal quenching

Received: April 20, 2022
Revised: June 14, 2022
Published online:

[1] A. H. Atabaki, S. Moazeni, F. Pavanello, H. Gevorgyan, J. Notaros, L. Alloatti, M. T. Wade, C. Sun, S. A. Kruger, H. Meng, K. Al Qubaisi, I. Wang, B. Zhang, A. Khilo, C. V. Baiocco, M. A. Popovic, V. M. Stojanovic, R. J. Ram, *Nature* **2018**, *556*, 349.
[2] R. Won, *Nat. Photonics* **2010**, *4*, 498.
[3] H. Subbaraman, X. Xu, A. Hosseini, X. Zhang, Y. Zhang, D. Kwong, R. T. Chen, *Opt. Express* **2015**, *23*, 2487.
[4] R. A. Soref, *Proc. IEEE* **1993**, *81*, 1687.
[5] R. Soref, *Adv. Opt. Technol.* **2008**, *2008*, 1.
[6] T. Wang, J.-J. Zhang, L. Huiyun, *Acta Phys. Sin.* **2015**, *64*, 204209.
[7] S. Takagi, R. Zhang, J. Suh, S.-H. Kim, M. Yokoyama, K. Nishi, M. Takenaka, *Jpn. J. Appl. Phys.* **2015**, *54*, 06FA01.
[8] Y. B. Bolkhovityanov, O. P. Pchelyakov, *Phys. Usp.* **2008**, *51*, 437.
[9] T. Komljenovic, M. Davenport, J. Hulme, A. Y. Liu, C. T. Santis, A. Spott, S. Srinivasan, E. J. Stanton, C. Zhang, J. E. Bowers, *J. Lightwave Technol.* **2016**, *34*, 20.
[10] F. A. W. Koch, B. R. Cohen, *Opt. Express* **2007**, *15*, 11225.
[11] R. E. Camacho-Aguilera, Y. Cai, N. Patel, J. T. Bessette, M. Romagnoli, L. C. Kimerling, J. Michel, *Opt. Express* **2012**, *20*, 11316.
[12] Z. Zhou, B. Yin, J. Michel, *Light: Sci. Appl.* **2015**, *4*, 358.
[13] A. J. Kenyon, *Semicond. Sci. Technol.* **2005**, *20*, R65.
[14] A. Polman, *J. Appl. Phys.* **1997**, *84*, 1.
[15] H. Ennen, G. Pomrenke, A. Axmann, K. Eisele, W. Haydl, J. Schneider, *Appl. Phys. Lett.* **1985**, *46*, 381.
[16] H. Ennen, J. Schneider, G. Pomrenke, A. Axmann, *Appl. Phys. Lett.* **1983**, *43*, 943.
[17] M. A. Lourenco, M. M. Milosevic, A. Gorin, R. M. Gwilliam, K. P. Homewood, *Sci. Rep.* **2016**, *5*, 37501.
[18] F. Priolo, G. Franzò, S. Coffa, A. Carnera, *Phys. Rev. B* **1998**, *57*, 4443.
[19] H. Wen, J. He, J. Hong, S. Jin, Z. Xu, H. Zhu, J. Liu, G. Sha, F. Yue, Y. Dan, *Adv. Opt. Mater.* **2020**, *8*, 2000720.
[20] J. Michel, J. L. Benton, R. F. Ferrante, D. C. Jacobson, D. J. Eaglesham, E. A. Fitzgerald, Y. H. Xie, J. M. Poate, L. C. Kimerling, *J. Appl. Phys.* **1991**, *70*, 2672.
[21] D. Eaglesham, J. Michel, E. Fitzgerald, D. Jacobson, J. Poate, J. Benton, A. Polman, Y. H. Xie, L. Kimerling, *Appl. Phys. Lett.* **1991**, *58*, 2797.
[22] H. Efeoglu, J. Evans, T. Jackman, B. Hamilton, D. Houghton, J. Langer, A. Peaker, D. Perovic, I. Poole, N. Ravel, *Semicond. Sci. Technol.* **1993**, *8*, 236.
[23] G. Van den Hoven, J. H. Shin, A. Polman, S. Lombardo, S. Campisano, *J. Appl. Phys.* **1995**, *78*, 2642.

© 2022 The Authors. Advanced Photonics Research published by Wiley-VCH GmbH

[24] F. Priolo, G. Franzò, S. Coffa, A. Polman, S. Libertino, R. Barklie, D. Carey, *J. Appl. Phys.* **1995**, *78*, 3874.
[25] X. H. Zhang, S. J. Chua, A. M. Yong, H. Y. Yang, S. P. Lau, S. F. Yu, X. W. Sun, L. Miao, M. Tanemura, S. Tanemura, *Appl. Phys. Lett.* **2007**, *90*, 013107.
[26] B. Ghosh, M. Takeguchi, J. Nakamura, Y. Nemoto, T. Hamaoka, S. Chandra, N. Shirahata, *Sci. Rep.* **2016**, *6*, 36951.
[27] H. C. Sio, D. Kang, R. Liu, J. Stuckelberger, C. Samundsett, D. Macdonald, *ACS Appl. Mater. Interfaces* **2021**, *13*, 32503.
[28] Y. Liu, M. R. Halfmoon, C. A. Rittenhouse, S. Wang, *Appl. Phys. Lett.* **2010**, *97*, 242111.
[29] F. Ren, J. Michel, D. Jacobson, J. Poate, L. Kimerling, *MRS Online Proc. Lib. (OPL)* **1993**, *316*, 493.
[30] P. Liu, J. P. Zhang, R. J. Wilson, G. Curello, S. S. Rao, P. L. F. Hemment, *Appl. Phys. Lett.* **1995**, *66*, 3158.
[31] X. D. Pi, C. P. Burrows, P. G. Coleman, *Phys. Rev. Lett.* **2003**, *90*, 155901.
[32] S. P. Jeng, T. P. Ma, R. Canteri, M. Anderle, G. W. Rubloff, *Appl. Phys. Lett.* **1992**, *61*, 1310.

© 2022 The Authors. Advanced Photonics Research published by Wiley-VCH GmbH